

---

# Development and Validation of an Advanced Low-Order Panel Method

---

Dale L. Ashby, Michael Dudley, Ames Research Center, Moffett Field, California  
Steven K. Iguchi, Sterling Federal Systems, Inc., Palo Alto, California

October 1988



National Aeronautics and  
Space Administration

**Ames Research Center**  
Moffett Field, California 94035



## SUMMARY

A low-order potential-flow panel code, PMARC, for modeling complex three-dimensional geometries, is currently being developed at NASA Ames Research Center. PMARC was derived from a code named VSAERO that was developed for Ames Research Center by Analytical Methods, Inc. In addition to modeling potential flow over three-dimensional geometries, the present version of PMARC includes several advanced features such as an internal flow model, a simple jet wake model, and a time-stepping wake model. Data management within the code has been optimized by the use of adjustable size arrays for rapidly changing the size capability of the code, reorganization of the output file and adopting a new plot file format. Preliminary versions of a geometry preprocessor and a geometry/aerodynamic data postprocessor are also available for use with PMARC. Several test cases are discussed to highlight the capabilities of the internal flow model, the jet wake model, and the time-stepping wake model.

## SYMBOLS

$B_{jk}$	velocity potential influence coefficient due to a uniform distribution of unit source on panel k
$C_{jk}$	velocity potential influence coefficient due to a uniform distribution of unit doublet on panel k
$c_p$	pressure coefficient
$D$	effective jet diameter
$DR$	decay rate constant for jet decay
$i, j, k$	unit vectors for rectangular coordinate system for velocity scan volume
$M$	number of rows on a patch
$N$	number of columns on a patch
$n$	total number of panels
$\mathbf{n}$	panel normal vector
$q_\infty$	free-stream dynamic pressure
$q(s)$	jet centerline dynamic pressure
$\mathbf{r}, \theta, z$	unit vectors for cylindrical coordinate system for velocity scan volume
$s$	arc length along jet centerline
$S$	total arc length along jet centerline
$T$	time
$V_j$	magnitude of the jet velocity
$V_\infty$	magnitude of the free-stream velocity
$\mathbf{V}_\infty$	free-stream velocity vector

$V_{\text{norm}}$	magnitude of prescribed velocity normal to a panel
$V_{\text{sf}}$	free-stream velocity scaling factor
$x, y, z$	global coordinates for paneled geometry, $x$ in free-stream flow direction
$\phi_{\infty}$	free-stream velocity potential
$\mu$	doublet singularity strength per unit area
$\sigma$	source singularity strength per unit area
Subscripts	
$j$	refers to panel $j$ or its control point
$k$	refers to panel $k$ or its control point
$\infty$	free-stream conditions

## INTRODUCTION

A potential flow panel code, called PMARC (Panel Method Ames Research Center), is currently being developed at NASA Ames Research Center to numerically predict flow fields around complex three-dimensional geometries. PMARC was derived from a low order panel code named VSAERO which was developed for NASA by Analytical Methods, Inc. PMARC contains many new subroutines which were written at Ames or by university faculty and students. The creation of PMARC was prompted by the need at Ames for a well-documented code, suitable for powered-lift aerodynamic predictions, with an open architecture which would facilitate making modifications or adding new features. An open code will allow other government agencies and contractors to make additional contributions to the code. A second objective in the development of PMARC was to create an adjustable-size panel code. This will allow PMARC to be tailored so an optimum match can be achieved between the computer hardware available to the user and the size of the problem being solved. Currently PMARC can be resized (i.e., the maximum number of panels can be changed) in a matter of minutes. PMARC can be run on computers ranging from a MacIntosh II workstation to a Cray X-MP. At its present state of development, PMARC contains several features considered to be state-of-the-art for panel methods. These include internal flow modeling for ducts and wind tunnel test sections, simple jet wake modeling essential for the analysis and design powered lift aircraft, and a time-stepping wake model which allows the study of unsteady motions. PMARC is a research tool that is envisioned as being in a continual state of development. Existing routines will be improved or replaced by new routines, and new features and options added as they become available.

One of the decisions that had to be made in the development of PMARC was the type of panel method to be used. Panel methods can be subdivided into two groups: low order and high order. In a low-order panel method, the singularities are distributed with constant strength over each panel. In a higher order method, the singularity strengths are allowed to vary linearly or quadratically over each panel. Higher order panel methods claim a better accuracy in the modeling of the flow field, but this is at the expense of increased code complexity and computation time. Experience with panel methods such as PANAIR, MACAERO, VSAERO, and QUADPAN, developed under NASA contracts and/or industry internal research

and development, has shown that low order methods can provide nearly the same accuracy as higher order methods over a wide range of cases; however, the computation time for low order panel methods is much shorter than for higher order panel methods<sup>1</sup>. Additionally, low order panel methods do not require exact matching between panels as higher order methods do. For these reasons, and to reduce program cost and complexity, the low order panel method was chosen for the basic methodology. The code is structured to accommodate the addition of a higher order solution method at a later date, if warranted.

To avoid unnecessary duplication of previous work, existing software was utilized whenever possible to reduce development time of PMARC and cost to the government. Of the several low order panel methods available, the 1000-panel version of VSAERO was felt to be the most robust, mature, and widely accepted by the engineering community. During its ten years of development by Analytical Methods Inc., which was supported largely by government and industry contracts, VSAERO has demonstrated that low order panel methods are a viable means of predicting aerodynamic flows about complex shapes. Two versions of VSAERO were delivered to Ames Research Center, one in 1982 and the other in 1985 under contracts NAS2-11169 and NAS2-11944, respectively<sup>2,3,4</sup>. The most recent was chosen as the initial framework and starting point in the development of PMARC.

Since the version of VSAERO delivered to the government was intended primarily as a demonstration and validation of a method, the code is structured so that it is extremely difficult to modify or replace any of its routines. This required as a first step the restructuring and modularizing of the code. The function of subroutines needed to be isolated and their interactions identified so that newly written or public domain routines could be added, and existing routines replaced.

This paper will discuss some of the advanced features available in the current version of PMARC. These include the internal flow model, the jet wake model, and the time-stepping wake model. In addition, the data management schemes used within the code and the preprocessing and postprocessing packages that are available for use with PMARC will be covered. Finally, several test cases will be presented which highlight some of the capabilities of PMARC.

## THEORY

### Potential Flow Model

Since VSAERO was used as the initial framework for PMARC, the potential flow theory on which PMARC is based is the same as that for VSAERO<sup>3</sup> and the Hess code from which it was derived<sup>5</sup>. The surface geometry is modeled in PMARC by dividing the surface into a set of quadrilateral panels. Each panel has a constant-strength source and doublet distributed over it. The source values are determined using the Neumann boundary condition shown in equation (1) at the panel control point.

$$\sigma = 1/4\pi * (V_{\text{norm}} - \mathbf{n} \cdot \mathbf{V}_{\infty}) \quad (1)$$

The normal velocity,  $V_{\text{norm}}$ , at the panel control point is either zero (no flow through the surface) or a user-defined value (to simulate suction or blowing) and the onset velocity vector is known. In PMARC, the onset velocity is a nondimensional unit vector. The doublet values are unknowns and are determined by using the matrix equation

$$[C_{jk}] [\mu_k] = [B_{jk}] [-\sigma_k] \quad (2)$$

where  $B_{jk}$  and  $C_{jk}$  are the panel source and doublet potential influence coefficients, respectively. The coefficient matrices  $[C_{jk}]$  and  $[B_{jk}]$  are square matrices of dimension  $n \times n$  where  $n$  is the number of panels used to model the geometry. The doublet potential influence coefficients for panels adjacent to wake separation lines will have the sum of the wake influence coefficients for the corresponding column of wake panels added to them<sup>3</sup>.

Because the matrix equation that must be solved can become very large (the influence coefficient matrix contains 1,000,000 elements for a 1000 panel case), a fast iterative matrix solver that solves line by line without requiring the whole matrix to be in memory at once was needed. PMARC makes use of a matrix solver that was written at NASA Ames Research Center by Charles Bauslicher. The matrix solver is based on an iterative scheme for computing the eigenvalues of large matrices<sup>6</sup>. The solver can handle matrices of the order of  $10^6 \times 10^6$ . Only two vectors at a time are needed in memory during the iterative solution process, allowing large matrices to be solved without requiring large amounts of



memory. This permits the solution of fairly complex problems (1000 to 4000 panels) on mini- and micro-class computers. The influence coefficient matrix and the right-hand-side vector remain on a disk scratch file. The solver requires the diagonal vector of the influence coefficient matrix and the right-hand-side vector to start the iterative process.

The convergence tolerance must also be passed to the solver. The convergence tolerance specified in PMARC is defined as the percent change in the solution vector elements between successive iterations, divided by 100. The element in the solution vector with the largest change is used to determine if the solution is converged or not. The cases which have been run to date using the solver in PMARC indicate that a convergence tolerance of 0.01 to 0.0005 will be adequate for most problems, although smaller convergence tolerances may be necessary for certain cases. The solver will generally converge to a solution in 50 to 75 iterations or less. A single iteration cycle is of the order of 0.0866 CPU seconds for 1000 panels and 0.695 CPU seconds for 4000 panels on the CRAY X-MP or 14.847 CPU seconds for 1000 panels and 119.154 CPU seconds for 4000 panels on a MicroVAX II. The current limit on number of solver iterations is 75. This limit could be raised if necessary, but the coding in the solver would have to be changed to fold the current set of vectors and matrix vector products to one and reset the dimension of the small matrix to 1 to prevent the disk scratch files and the input/output times from becoming too large<sup>6</sup>.

### Internal Flow Modeling

The code PMARC currently supports modeling of internal flows. This is accomplished by modeling the internal flow geometry as a closed box with the panel normal vectors pointing into the interior of the box. Inflow and outflow to the box (flow through a duct) may be prescribed as normal velocities on groups of panels. The inflow and outflow must be prescribed so that the continuity equation is satisfied. The internal flow geometry can be a simple empty duct, or it may contain other objects such as wings or vanes to simulate a test article in a wind tunnel test section.

For internal flows, the doublet influence coefficient matrix is singular in its conventional form<sup>7</sup>. This is because the potential function for internal flow geometries is known only to within an arbitrary constant, whereas for external flow geometries the

arbitrary constant is determined by the potential at infinity ( $\phi_\infty$ ). In order to circumvent this problem, the potential (or a doublet value) must be specified somewhere on the geometry as a boundary condition. Normally, the source values for all the panels are known on a geometry from the Neumann boundary condition and the doublet values are solved for as in equation (2). For internal flows, the matrix singularity can be eliminated by arbitrary specification of a known doublet value, usually zero, on one panel. In the matrix equation, this known doublet value is substituted into equation (2) and the corresponding source value on the panel is treated as an unknown. Assuming the known doublet value is specified on the first panel, equation (2) can be rewritten to yield

$$\begin{array}{ccccccccc}
 B_{11} & C_{12} & C_{13} & \dots & \sigma_1 & = & C_{11} & B_{12} & B_{13} & \dots & -\mu_1 \\
 B_{21} & C_{22} & C_{23} & \dots & \mu_2 & = & C_{21} & B_{22} & B_{23} & \dots & -\sigma_2 \\
 B_{31} & C_{32} & C_{33} & \dots & \mu_3 & = & C_{31} & B_{32} & B_{33} & \dots & -\sigma_3 \\
 \vdots & \vdots & \vdots & \vdots & \vdots & & \vdots & \vdots & \vdots & \vdots & \vdots \\
 \vdots & \vdots & \vdots & \vdots & \vdots & & \vdots & \vdots & \vdots & \vdots & \vdots \\
 \vdots & \vdots & \vdots & \vdots & \vdots & & \vdots & \vdots & \vdots & \vdots & \vdots
 \end{array} \quad (3)$$

The solution of equation (3) results in a new, and possibly incorrect, source value for the panel on which the doublet is prescribed. Once the matrix solution is obtained, the source value that was obtained from the matrix solution is replaced by the original correct source value which satisfied the Neumann boundary condition from equation (1). This procedure allows the solution of an otherwise indeterminate matrix.

The panel used for the specified doublet has an impact on the convergence of the solution. Usually the best convergence is obtained if this panel is placed near the end of the matrix (i.e. the last panel). The doublet value used also affects convergence. It is best to use a doublet value which is close to the doublet strengths on the neighboring panels. The first run can be made with the assigned doublet value set to zero. If there is a significant discrepancy between the assigned doublet value and the doublet values on the neighboring panels, the assigned doublet value can be set to the weighted average of the doublet values on the neighboring panels and the calculation rerun. There will be some velocity anomalies immediately adjacent to the doublet specification panel due to inexact matching of the doublet strengths, but this has a negligible effect on the overall solution if the panel chosen is far from the primary regions of interest.

In internal flow problems, there is a certain amount of "leakage" in or out of the internal flow geometry due to the Neumann boundary condition for each panel being imposed only at panel control points<sup>8</sup>. The "leakage" from an internal flow geometry can be minimized by applying a scaling factor,  $V_{sf}$ , to the unit onset vector, thereby changing the source values that are computed in equation (1). Thus for internal flow problems, equation (1) can be rewritten as follows.

$$\sigma = 1/4\pi * (V_{norm} - \mathbf{n} \cdot (V_{sf} * V_{\infty})) \quad (4)$$

Since the source values change when  $V_{sf}$  is applied, the computed doublet values also change since the source values form the right-hand-side of equation (2). Scaling the onset velocity vector effectively reduces the jump in potential across the panels and hence the doublet strengths, producing a more stable solution<sup>8</sup>. The scaling factor  $V_{sf}$  is normally set to a value between zero and one and is adjusted until conservation of mass is achieved within the internal flow geometry. Conservation of mass may be determined by looking at inflow and outflow velocity specifications and the velocities at different cross sections of the geometry.

A far field approximation is used in computing all the influence coefficients. A far field radius is computed for each panel. This far field radius is equivalent to a user-defined far field factor which is constant for all panels, multiplied by a panel characteristic length. Inside the far field radius, the panel is treated as having distributed singularities on it, whereas outside the far field radius the panel is treated as having point singularities on it. The setting of the far field factor also affects the continuity condition of an internal flow problem<sup>8</sup>. By using a larger far field factor, a smaller  $V_{sf}$  can be chosen to achieve continuity in the internal flow. This is because with a larger far field factor, more panels are treated as having distributed sources and doublets instead of point sources and doublets. This reduces the "leakage" from the internal flow model. Unfortunately it also increases computation time for a solution. The larger far field factor also yields more accurate velocity computations within the internal flow. A tradeoff between solution time and accuracy required must be made in setting the value of the far field factor. If no velocity calculations are required, (i.e., no scan planes, off-body streamlines, or wake relaxations) then the default value of 5.0 for the far field factor is probably adequate. Larger values (on

the order of 10.0 or greater) should be considered if velocity computations are to be made.

### Jet Modeling

The PMARC code offers a simple potential-flow jet model which will predict the gross effects on the flow field of a jet in crossflow. The jet wake model in PMARC does not currently model any entrainment into the jet and it does not model the jet/surface interactions very accurately. It does predict the jet trajectory under the influence of the free-stream velocity and the velocities induced by the body, the degeneration of the jet into a pair of vortices, and the decay of the jet centerline velocity with distance along the jet.

Generation of the initial jet wake geometry is similar to the method described in reference 4. Jets are modeled by separating a closed wake doublet sheet from a paneled jet stub which represents the potential core of the jet. The jet stub shape should be cylindrical with a cross section that matches the jet exit shape. The jet stub should be attached at one end to the physical jet exit (i.e., to the surface from which the jet is issuing). The other end of the jet stub should be capped off with a flat patch which has a normal velocity (representing the jet exit velocity) specified on it. The length of the jet stub can be set to match experimental data for the length of the potential core of a jet; however, it should not be any shorter than two jet diameters in length to ensure that the proper circulation is developed around the jet stub.

The initial jet centerline trajectory is established automatically by using Margason's empirical formula for trajectory of a jet in crossflow<sup>9</sup>. The jet centerline is established in a local ( $x/D$ ,  $z/D$ ) coordinate system with the  $z/D$  axis being normal to the jet exit plane and the free-stream velocity vector lying in the ( $x/D$ ,  $z/D$ ) plane. The automatically generated jet trajectory coordinates can be optionally written to a file in global ( $x$ ,  $y$ ,  $z$ ) coordinates for editing and subsequent manual input of the jet trajectory. This is useful if the automatically generated jet runs into other objects. The PMARC code allows jets with deflection angles from  $0^\circ$  to approximately  $\pm 150^\circ$  to the free-stream velocity vector. Beyond a  $150^\circ$  deflection angle, Margason's equation becomes inaccurate.

Jet grid planes are then generated normal to the jet trajectory. The  $x$  position of the last jet grid plane is set in the input deck and the jet grid planes are distributed in equal ( $z/D$ ) increments along

the jet trajectory. This makes the grid-plane spacing dense near the jet exit and sparse at the end of the jet. The initial jet wake shape is generated by copying the jet exit shape to each of the jet grid planes and creating panels between the jet grid planes.

The doublet strengths that are shed into the first row of jet wake panels are determined by the jump in doublet strength across the separation line. The separation line for the jet wake is defined as the edge of the row or column of panels to which the jet wake is attached on the jet stub. Each column of jet wake panels is attached to a pair of separation panels (whose common side define the separation line) on the jet stub. The difference in the doublet strengths on the pairs of separation panels is the doublet strength that is shed into the first panel on each column of jet wake panels. Thus the doublet solution on the jet stub model determines the doublet strengths shed into the jet wake.

The variation in doublet strength in the peripheral direction on the jet wake is dependent on the circulation developed by the flow past the jet stub. The peripheral variation in doublet strength is maintained constant down the length of the jet. During jet wake relaxation, it is this peripheral variation in doublet strength which leads to the rollup of the jet wake into the vortex pair commonly observed in experimental investigations<sup>10</sup>.

The initial doublet gradient in the streamwise direction on the jet wake is established as the jet exit velocity minus the component of the free-stream velocity in the jet direction. The doublet gradient is then decayed exponentially along the jet trajectory using the equation

$$d\mu/ds = d\mu/ds|_{s=0} * e^{(-S/DR)} \quad (5)$$

where  $d\mu/ds|_{s=0}$  is the initial doublet gradient at the jet exit,  $S$  is the distance along the jet trajectory to the last jet grid plane, and  $DR$  is the decay factor. This allows the simulation of jet velocity (and hence dynamic pressure) decay along the jet trajectory, since velocity is equal to the doublet gradient. The decay rate of the doublet gradient is set automatically in the code to decay the jet velocity to free-stream velocity at the end of the jet. Thus the decay rate of the jet velocity can be controlled by changing the length of the jet. Alternatively, the automatic decay rate value can be

overridden by replacing the default with a nonzero value for the decay rate.

The jet relaxation scheme used in PMARC provides a stable means of relaxing the jet shape and the jet trajectory under the influence of both the free-stream velocity and any paneled surfaces. The jet wakes are relaxed at two levels. The first or inner level of relaxation is a fast relaxation step. A new potential solution is not computed after each fast relaxation step. The second or outer level of relaxation is a normal relaxation step where a new potential solution is formed after each step. The fast relaxation steps are made after each normal relaxation step. By using an appropriate combination of fast and normal relaxation steps, the jet relaxation process can be sped up significantly. Generally two or three fast relaxation steps can be made for each normal relaxation step without the relaxation process becoming unstable.

The jet relaxation procedure in PMARC uses a quasi-time step to control the relaxation. Figure 1 shows an overview of the details of the relaxation scheme. The arclength to each grid plane along the jet trajectory and the average jet velocity at each jet grid plane are calculated. The jet velocities are obtained by differentiating the doublet strength between adjacent jet wake panels in the "jetwise" direction on each column around the periphery of the jet and averaging the resultant velocity values at each grid plane. This method provides a quick, reliable way of obtaining the jet velocities all along the jet trajectory. Once the arclength to each jet grid plane and the jet velocity at each grid plane are known, a total time to reach the jet grid plane is then computed, assuming time  $(T)=0$  at the jet exit. The number of time steps that are taken between consecutive jet grid planes in relaxing the jet wake is set in the input file. The total number of time steps required to reach a given jet grid plane is equal to the grid plane number multiplied by the number of time steps between consecutive grid planes. The total time required to reach each jet grid plane from the jet exit plane is then divided by the total number of time steps required to reach that jet grid plane from the jet exit. This yields the time step for each grid plane.

The actual relaxation procedure steps through one jet grid plane at a time, starting at the first grid plane following the jet exit and going to the end of the jet. The velocity is computed at all the jet wake corner points on a jet grid plane. The velocity calculation is

made using the influence coefficients and the source and doublet strengths of all the panels in the geometry and wakes. The jet wake corner-point velocities are then converted into the local jet grid-plane coordinate system. Each corner point on a grid plane is moved in the direction of the in-plane component of velocity by a distance equal to the in-plane component of the velocity at that corner point, multiplied by the time step for that grid plane. When all the corner points on a jet grid plane have been moved, the run-time counter is incremented by the time step for that grid plane and the calculations proceed to the next grid plane until the end of the jet wake is reached. This completes one relaxation step in jet relaxation. During the relaxation process, if the run-time counter is equal to or greater than the total time for a jet grid plane, that grid plane is fully relaxed and will be skipped on subsequent relaxation steps. A user-defined expansion function for the jet wake can be input. The expansion is applied to the jet wake after it has been relaxed.

### Time-stepping Wake Model

In the PMARC code, the wake generation and relaxation schemes used in the 1000-panel VSAERO code have been replaced with a time-stepping wake model. The time-stepping wake scheme in PMARC is based in concept on the pilot version of the time-stepping routines written by Dr. Joseph Katz of San Diego State University which were coupled with the 1000-panel VSAERO code and tested with favorable results<sup>11</sup>. The time-stepping routines allow the user to specify a prescribed motion for the paneled geometry. The wakes from the paneled geometry are then developed over a series of time steps with the wake trajectory and shape reflecting the motion of the paneled geometry. The time-stepping routines allow either unsteady or steady motions to be prescribed. The time-stepping wake makes it possible to compute aerodynamic data for complete aircraft configurations going through maneuvers.

### DATA MANAGEMENT

One of the keys to the success or failure of any numerical method is how well data is managed within the code. In a panel code there are many large arrays and blocks of data that need to be manipulated within the code as well as written to output and plot files. If a good data management scheme is not implemented within the code, the code can quickly become too large, inefficient, and slow to be of any use. A data management scheme has been devised for PMARC which seeks to maximize the number of panels the code can

handle while minimizing the amount of memory and disk scratch space required to run the code. Specific aspects of the data management scheme include use of variable dimensioning for all major arrays within the code, creation of a memory-saving common block in which to store arrays local to a subroutine, provision of a reasonable balance between the amount of memory used and the amount of disk scratch space used, and elimination of redundancy of variables both within the code and in the plot and output files.

### Code Sizing

The PMARC code has adjustable arrays for all the geometry, wake, and solution related arrays. A core set of parameter statements are defined in a parameter file, shown in appendix A. This core set of parameter statements controls the sizing of all major arrays in the code. Parameter statements within each subroutine are then set by using the values defined in the parameter file. Integer limits for variables and loops within the code are all defined in data statements in a data file, also shown in appendix A. This procedure allows the user to change all array sizes and limits in the code from two small files. It also eliminates the possibility of forgetting an array or limit in the redimensioning process. Thus the size of the code (i.e., the number of panels it can handle) can be changed from several hundred to 10 or 20 thousand or more in a manner of minutes.

The main limitation on the number of panels the code can handle is the amount of memory and disk space available on the machine on which the code is being run. The current version of PMARC can be run with 3000 panels on a MicroVAX II with 3 Mb of memory and 210 Mb of disk space. PMARC has been run on the Cray X-MP with as many as 6000 panels without any problem. A modified version of PMARC has even been run with 1000 panels on a MacIntosh II with 2.5 Mb of memory and 20 Mb of disk space. By selectively changing certain parameters, the user can increase the capacity of one particular part of the code, say the number of patches or wakes allowed, without having to increase the capacity of the entire code. This allows the user to customize the size of the code to fit his particular needs and hardware capacity.

The parameter file is compiled and linked into PMARC using INCLUDE statements in each subroutine. The data file is compiled and linked into PMARC with an INCLUDE statement used in the PMARC module only. Then the data is passed to the other



subroutines through a common block. The Cray X-MP does not support the INCLUDE statement, so the parameter and data files are actually included as part of each subroutine for the Cray version of PMARC. Other machines not supporting the INCLUDE statement would need to use the Cray version of PMARC.

With the advent of relatively inexpensive memory for modern computers, it has become less necessary to use disk scratch space to conserve memory. Even small PCs usually have at least 1 Mb of internal RAM and can be expanded to 4 or 8 Mb. In developing PMARC, many of the disk scratch files were removed that were used in the 1000-panel VSAERO to conserve memory. Removal of the disk IO statements and use of common blocks instead to pass information between subroutines greatly streamlines the coding and produces a faster-running code. During the process of implementing the adjustable arrays in PMARC, a common block was set up in each subroutine that is used solely to conserve memory. The memory-saving common block is used as a common memory space to store large arrays, but not to pass anything between subroutines. Thus care must be taken not to include anything in the memory-saving common block that is to be passed through the common blocks to other subroutines.

### Output File

The aerodynamic data section of the output file from PMARC has been reorganized to add new options to the panel aerodynamic data printout and to separate the force and moment data out from the panel aerodynamic data. Once the doublet solution has been found, the doublets on the surface are numerically differentiated to give the surface velocity components. From the velocities, the pressure coefficient and the local Mach number at each panel centroid is computed. The panel number, control point location, doublet value, velocity components, velocity magnitude, pressure coefficient, and local Mach number are then written to the output file for each panel. Velocity data can be displayed in a variety of different units or in nondimensional form. For reference, the velocity units and the free-stream velocity are written to the output file at the beginning of each column on each patch.

Forces and moments are summed up, panel by panel, for each patch, component, assembly, and the whole model. Forces and moments are also summed up for each column of panels on user-specified patches to give section coefficients. The summed forces and

moments are put in coefficient form and are transformed to wind, stability, and body axes. The section coefficients are written to the output file in wind, stability, and body axes, after each column of aerodynamic data for the patches on which they were computed. The patch, component, assembly, and total force and moment coefficients are written to the output file in wind, stability, and body axes, after the panel aerodynamic data for all the patches has been written. The patch wetted area, nondimensionalized by the reference area, is also written at this time. For the case where a plane of symmetry about  $y=0.0$  was used, the patch, component, and assembly force and moment coefficients are for the paneled geometry only. The total coefficients include the contribution of the reflected image.

### Plot File

The PMARC plot file is designed to contain as much information as possible regarding geometry and aerodynamic data in as compact a space as possible. The idea is to let PMARC do the computing and have the plotting package process and display the information. Computing should be kept to a minimum within the plotting package to keep its speed high. The general blocking of the data within the PMARC plot file is shown in figure 2. The geometry data is written to the file first. The geometry data is outside the wake and boundary layer iteration loops since the geometry data will not change from iteration to iteration. A block of wake and aerodynamic data is written for each wake iteration. On-body streamline data and boundary layer data are appended to the wake and aerodynamic data block following the completion of the wake iteration loop. After the completion of the boundary layer loop, the off-body velocity scan and off-body streamline data are written. The plot file is keyed or indexed at each wake iteration, at each boundary layer iteration, at the off-body velocity scan data, and at the off-body streamline data. This allows the plotting package to key to a specific block of data for plotting without having to read in the entire plot file.

The numbering sequence for rows, columns, panels, and corner points on a surface patch is shown in figure 3. The arrangement of the geometry data block is as follows. The first record contains the total number of patches in the geometry. This is followed by a set of records containing patch number, patch name, number of columns and rows, and first and last panel number on each patch. The next record contains the total number of panels in the geometry. Next,

panel information is written, stepping through each patch, each column on each patch, and each row on each column. Each record consists of the (x, y, z) coordinates of the first corner point of each panel, the coordinates of the panel centroid, and the panel normal vector at the panel centroid. At the end of each column of panels, an extra record must be included which contains the coordinates of the second corner point of the last panel in the column. After the data for the last column of panels has been written, an extra set of records is included to write the fourth corner point of the panels in the last column and the third corner point of the last panel in the last column. In this fashion all the corner points, centroids, and normal vectors are written to the plot file for each panel on each patch with no duplication within a patch. Following the corner point, centroid, and normal data is the panel neighbor data. Each record contains the neighbor panel number and the side of that neighbor panel adjacent to a given panel for each of the four sides of that panel.

Following the geometry data block is the wake data block. The wake data is written to the plot file in the same way as the geometry data. The only exceptions are that wake number replaces patch number and neighbor data is not written for wake panels. Thus the wake data includes wake panel corner points, centroids, and normal vectors.

The aerodynamic data block is written next. Aerodynamic data is written at the panel corner points and at the centroids using the same logic that is used to write the geometry and wake data. The aerodynamic quantities that are written to the plot file are doublet strength, the (x, y, z) components of velocity, the velocity magnitude, the pressure coefficient, and the local Mach number at each panel corner point and centroid.

The remainder of the data written to the plot file consists of optional data blocks. These include on-body streamline data, boundary layer data, off-body velocity scan data, and off-body streamline data. The on-body and off-body streamline data include the number of lines, the number of points on each line, the (x, y, z) location of each point, the three velocity components and the velocity magnitude, the pressure coefficient, the local Mach number, and the arclength at each point on each streamline. The boundary layer data consist of the number of lines, the number of points per line, the (x, y, z) location of each point, the streamwise velocity magnitude, the boundary layer thickness, the momentum thickness, the

displacement thickness, the shape factor, the Reynolds number based on momentum thickness, the skin friction coefficient, and the arclength at each point. The off-body velocity scan data consists of the number of volumes, the number of points in the (i, j, k) directions within each volume, and the volume type. For each scan point the (x, y, z) location, the velocity components and magnitude, the pressure coefficient, and the local Mach number are written.

### Geometry Preprocessing Package

The preprocessing package that has been put together for PMARC is based primarily on PANEL, a code written by George Howell of General Dynamics under contract NAS2-11958<sup>12</sup>. PANEL has been modified to use adjustable arrays, so it can be sized to match PMARC. PANEL can read in an existing PMARC, VSAERO, or PANAIR input deck or can be used to create a new input deck. PANEL allows the user to interactively modify panel densities, remove rows or columns, reverse patches, drop patches, create intersections between patches, create cutouts, and scale, translate, or rotate a patch. PANEL has its own graphics package to display geometry on a terminal screen so the user can see the changes that have been made. Once the user has finished defining or modifying the geometry for a given job, PANEL creates an input deck with geometry definition in terms of panel corner points in global coordinates. PANEL currently outputs only the geometry section of the input deck and does not affect wakes or special options.

### Geometry/Aerodynamic Data Postprocessor

A sophisticated new postprocessing package is being written by Sterling Software to process the plot file that PMARC writes. The postprocessing package, called PAD (Plot Aerodynamic Data), is supported by the ASP graphics package which was written and is supported at Ames. PAD makes use of variable dimension arrays and uses the same parameter file that PMARC uses to size the arrays. This allows PAD to be sized for any total number of panels the user wants, similar to PMARC. This is particularly convenient for transporting PAD to smaller machines where memory and disk space become constraints. There are two versions of PAD, one for the VAX computer and one for the IRIS workstation. Both the VAX version and the IRIS version of PAD are currently being developed. Preliminary releases are available for both versions. The IRIS version currently handles only the geometry data. The options for handling the aerodynamic data remain to be added.

The VAX version of PAD is written in standard Fortran and is written to be as portable as possible to other machines. PAD supports a variety of output devices, including Tektronix terminals and Tektronix emulators, Versatec printers, laser printers, and Dicomed. PAD is menu-driven, with default answers used wherever possible. A new default answer set can be optionally created, allowing the default answers to be customized for particular applications. PAD can be run as a batch job and will create a device independent (DIP) file which can then be processed for the appropriate output device. Full error handling exists within the program. The user input for creating the current plot on a CRT screen can be saved to create a DIP file for obtaining a hardcopy of the plot. PAD provides full rescaling and clipping of plots. PAD has the capability of reading in data from several different PMARC plot files and can overlay geometric or aerodynamic plots. The information that PAD can process is broken up into three different areas: the geometry and wake information, the on-body aerodynamic data, and the off-body aerodynamic data.

The PAD program can plot three-dimensional wire frame models from a user-defined viewpoint outside the body. The viewpoint can be specified as coordinates in three-dimensional space or as a combination of coordinates and rotations about a specified axis. PAD also allows the plotting of two-dimensional cross section outlines generated by an arbitrary plane cut through the three-dimensional model. The plotting of reflected geometries when only half the geometry is modeled is supported by PAD. The geometry plot can be limited to specific panel ranges or patches. Wakes can be optionally included in the geometry plot and can be limited to particular wakes or panel ranges within selected wakes. PAD supports three-dimensional wire frame plots with hidden lines removed. PAD allows the whole geometry or portions of the geometry to be translated an arbitrary distance in an arbitrary direction.

The VAX version of PAD can plot  $V_x$ ,  $V_y$ ,  $V_z$ ,  $V$ ,  $c_p$ , and Mach number versus  $x$ ,  $y$ ,  $z$ , or arc length at the intersection between a user-specified cutting plane and the model. If the cutting plane does not intersect the model at the control points or the corner points of panels on the model, PAD will perform a linear interpolation to obtain the aerodynamic data at the intersection points upon user request. Otherwise PAD will select the closest data point to the intersection point and use that. The two-dimensional cross section

outline can be optionally superimposed on the data plot. Experimental data, obtained either interactively or from a data file, can also be included in the aerodynamic data plot. PAD can plot on-body streamlines on user-defined views of the body. Any streamlines hidden by the body in a given view can be optionally removed. Aerodynamic data variation along a streamline can be plotted versus  $x$ ,  $y$ ,  $z$ , or arc length. The aerodynamic data on the on-body streamlines can include boundary layer parameters if boundary layer iterations were made.

The off-body aerodynamic data that PAD can process includes off-body velocity scans and off-body streamlines. Velocity scan data can consist of points, lines, planes, and volumes. PAD allows the user to select the points, lines, or planes for plotting and provides either contour plots (only for planes) or vector plots of aerodynamic data. In the general case of a scan volume, the user can select either  $i$ ,  $j$ , or  $k$  as the direction for line plots and any combination of a pair of  $i$ ,  $j$ ,  $k$  directions for plots on a plane. This allows random access to lines and planes in any of the three primary directions within the scan volume. For cylindrical volumes, the three directions become  $r$ ,  $\theta$ , and  $z$ . Plots on curved planes are currently plotted on the projected plane. Off-body streamlines can be plotted on a user-defined view of the body and parts of the streamlines hidden by the body can be optionally clipped. As with the on-body streamlines, aerodynamic data on the streamlines can be plotted versus  $x$ ,  $y$ ,  $z$ , or arc length.

The IRIS version of PAD will accept the same PMARC plot file that the VAX version does. The IRIS version does not support all the two-dimensional plots that the VAX version does. The IRIS version was written primarily to take advantage of the three-dimensional plotting, shading, and color options of the IRIS, as well as the mouse manipulation of items on the screen that the IRIS provides. The IRIS version of PAD can plot three-dimensional wire frame models of the geometry and the wakes. As with the VAX version, selected patches or panel ranges for geometry and selected wakes, panel ranges, or no wake plotting for the wakes can be specified. Once the geometry and wakes are plotted on the screen, the viewpoint can be manipulated by simply moving the mouse. Both translations and rotations are supported and the viewpoint can be either inside or outside the body. Once the desired viewpoint is found, the geometry can be shaded to create a solid. The user can specify the desired colors for the different panel groups or patches within the geometry. Wakes

can also be shaded and colored, but the wakes will be made semi-transparent if they are shaded so that geometry that might be obscured by a wake can be seen.

## TEST CASES

### Internal Flow Test Case

A sample internal flow problem is shown in figure 4. The geometry consists of the contraction, test section (including acoustic liner), and primary diffuser of the 40-by-80-foot circuit of the National Full-Scale Aerodynamics Complex (NFAC) at NASA Ames Research Center. The tunnel was modeled using 44 panels equally spaced circumferentially around the tunnel and 109 panels in the axial direction. The panel spacing along the axis of the tunnel was made dense in regions of high curvature (i.e., the contraction) and in the region where the solution is of most interest (i.e., the test section). A total of 5208 panels were used for the tunnel model. The tunnel test section velocity was used as the reference velocity and the inflow and outflow velocities to the tunnel were set to yield a nondimensional test section velocity of 1.0. The value of  $V_{sf}$  was set to 0.26 and the far field factor was left at its default value of 5.0 for this case.

Figure 5 shows the pressure coefficients on the tunnel walls as computed by PMARC for the entire length of the tunnel. Figure 6 shows a comparison between pressure coefficients computed by PMARC and pressure coefficients measured in the test section of the tunnel during the flow calibration test of the facility. The PMARC computations agree well with the experimental data. The pressure spikes at the entrance and exit ramp of the acoustic liner in the test section shown in the PMARC results do not appear in the experimental results because no experimental data is available on the entrance and exit ramps.

### Jet Test Cases

Several simple jet test cases were run to verify the jet model in PMARC. Figure 7 shows the initial jet wake geometry generated for a jet with a velocity ratio of 8.0 inclined  $90^\circ$  to the free-stream velocity vector. For simplicity, the jet is modeled as exiting from the base of an inverted cone. The jet stub is modeled as a circular cylinder with 16 panels equally spaced around its perimeter and four equally spaced divisions along its length. The length of the jet

stub is approximately 3.0 jet diameters. The top of the jet stub is closed off with a flat circular patch on which a normal velocity (representing the jet exit velocity) is specified. The jet wake is attached to the top of the jet stub. Thirty jet grid planes were used for this jet wake, with the last jet grid plane being approximately 20 jet diameters downstream of the jet exit measured along the jet centerline.

The computed jet dynamic pressure decay is compared with experimental data for a jet issuing from a flat plate<sup>13</sup> in figure 8. The region of constant dynamic pressure in the jet between  $s/D=0.0$  and  $s/D=3.0$  is the potential core of the jet and is modeled in PMARC by the jet stub. The length of the potential core varies with jet velocity ratio<sup>13</sup>. The length of the jet stub in the calculation has been adjusted to match the length of the potential core in the experimental data. From figure 8 it can be seen that the exponential decay scheme used in PMARC provides a reasonable first order approximation to jet dynamic pressure decay.

Figure 9 shows the jet wake from figure 7 after it has been relaxed by eight relaxation steps (four normal relaxation steps and two fast relaxation steps per normal relaxation step). Only the jet cross sections are plotted so that the details of the jet shape are more easily seen. The first four jet grid planes have been fully relaxed. The remaining jet grid planes are only partially relaxed. The characteristic kidney shape of the jet is clearly visible as the jet wake degenerates into a pair of vortices. In these cases, further jet wake relaxation is not warranted as the trajectory of the jet will not change appreciably. If the jet is relaxed further, the shape of the jet will become unstable near the end of the jet because all the panel edges in the "jetwise" direction coalesce into the vortex pair. Figure 10 shows the jet wake from figure 9 after an empirical jet expansion function has been applied to the jet. Figures 11 and 12 show velocity scans through the jet wake at  $s/D=1.15$  and  $s/D=25.0$ , respectively. The simulation of the vortex pair can be clearly seen.

Figures 13 through 15 show jets with deflection angles of  $0^\circ$ ,  $60^\circ$ , and  $120^\circ$  to the free-stream velocity. The jet wake with a deflection of  $0^\circ$  to the free-stream velocity was not relaxed. Because it is already parallel to the free stream, the trajectory of the jet and the jet shape will not change with relaxation. If there were other surfaces near the jet path (i.e., wings or bodies), then jet wake relaxations would have to be performed since the objects would



affect the trajectory of the jet. The jet wakes with deflection angles of  $60^\circ$  and  $120^\circ$  were relaxed a total of eight relaxation steps ( four normal relaxation steps and two fast relaxation steps per normal relaxation step). The rollup of the jet wake into a vortex pair is evident in both cases.

### Time-stepping Wake Test Case

A simple test case for which the qualitative results are known was run to initially check out the time-stepping wake model in PMARC. The test case chosen was a symmetric airfoil wing at zero angle-of-attack in forward flight performing a constant rate roll. The wing used for this test case was a NACA 0012 section wing with an aspect ratio of five. The wing was modeled using 15 panel divisions in the chordwise direction on the upper and lower surfaces (for a combined total of 30 panel divisions in the chordwise direction) and 20 panel divisions in the spanwise direction. Panel spacing in both the chordwise and spanwise directions was full cosine spacing, yielding denser paneling at the leading and trailing edges and at the wing tips. The tips of the wing were closed off with semicircular caps. A total of 690 panels were used to model the wing. The test case was run for a total of 20 time steps, with a roll rate of  $3^\circ/\text{second}$ ,  $V_\infty = 1.0 \text{ ft/second}$ , and a time step of 2 seconds.

Figure 16 shows the wake development after the wing has rolled  $90^\circ$ . The rollup of the wake at the edges due to the tip vortices can be clearly seen. Figure 17 shows the spanwise pressure distribution on the upper and lower surfaces of the wing at  $x/c = 0.25$ . As expected, the pressure distribution on the rising half of the wing (positive  $y$ ) is equal and opposite to the pressure distribution on the falling half of the wing. Although this simple test case illustrates the functionality of the time-stepping wake model, a more complete checkout of the time-stepping routines and comparison with experimental data remains to be done.

### CONCLUDING REMARKS

The development of an advanced low-order potential-flow panel code, PMARC, for modeling complex three-dimensional geometries has been outlined. Several of the advanced features currently included in the code, such as internal flow modeling, a simple jet wake model, and a time-stepping wake model, have been discussed in some detail. The capabilities of these features has been demonstrated by some simple test cases. Additionally, the data

management schemes used within PMARC were outlined. The adjustable size arrays used in PMARC allow the code to be sized to the particular problem being solved and the computer hardware being used. The new plot file format and the geometry preprocessor and geometry/aerodynamic data postprocessor allow the user great flexibility in manipulating and analyzing the large amount of data that can be generated by PMARC.

Many refinements still need to be pursued for the PMARC code. Among these would be automating the setting of the scaling factor  $V_{sf}$  for internal flow problems so that the user does not have to make several runs of the code to set this parameter. Some sort of entrainment model needs to be included in the current jet wake model to better simulate the physics of a jet wake. The capabilities of the time-stepping wake model need to be extended to handle cases with relative component motion, such as rotor rotation relative to a moving helicopter fuselage. The open architecture of the code and the programming standards adhered to within the code should make it easier to make these refinements and to add new features to the code in the future.

## REFERENCES

1. Margason, R. J., Kjelgaard, S. O., Sellers, W. L., Morris, C. E. K., Walkey, K. B., Shields, E. W.: Subsonic Panel Methods - A Comparison of Several Production Codes, AIAA Paper 85-0280, Jan. 1985.
2. Maskew, B.: Program VSAERO, A Computer Program for Calculating the Nonlinear Characteristics of Arbitrary Configurations, Users Manual, NASA CR-166476, Dec. 1982.
3. Maskew, B.: Program VSAERO, A Computer Program for Calculating the Nonlinear Characteristics of Arbitrary Configurations, Theory Document, NASA CR-4023, Sept. 1987.
4. Maskew, B., Strash, D., Nathman, J., Dvorak, F. A.: Investigation to Advance Prediction Techniques of the Low-Speed Aerodynamics of V/STOL Aircraft, NASA CR-166479, Feb. 1983.
5. Hess, J. L.: Calculation of Potential Flow About Arbitrary Three-Dimensional Lifting Bodies, McDonnell Douglas Corp. Rep. No. MDC J5679-01, Oct. 1972.
6. Davidson, E. R.: The Iterative Calculation of a Few of the Lowest Eigenvalues and Corresponding Eigenvectors of Large Real-Symmetric Matrices, J. Comp. Phys. 17, 1975, pp. 87-94.
7. Hunt, B.: The Panel Method for Subsonic Aerodynamic Flows: A Survey of Mathematical Formulations and Numerical Models and an Outline of the New British Aerospace Scheme, Von Karman Institute for Fluid Dynamics, Lecture Series 1978-4, vol. I, March 13-17, 1978.
8. Ashby, D. L., and Sandlin, D. R.: Application of a Low Order Panel Method to Complex Three-Dimensional Internal Flow Problems, NASA CR-177424, Sept. 1986.
9. Margason, R. J.: The Path of a Jet Directed at Large Angles to a Subsonic Free Stream, NASA TN D-4919, Nov. 1968.

10. Kamotani, Y. and Greber, I.: Experiments on a Turbulent Jet in a Cross Flow, NASA CR-72893 FTAS/TR-71-62, June 1971.
11. Katz, J., and Maskew, B.: Unsteady Low-Speed Aerodynamic Model for Complete Aircraft Configurations, AIAA Paper 86-2180, Aug. 1986.
12. Howell, G. A.: Automated Surface and Plume Simulation Procedure for Use with Aerodynamic Panel Codes, NASA CR-177420, May 1986.
13. Kuhlman, J. M., Ousterhout, D. S. and Warcup, R. W.: Experimental Investigation of Effect of Jet Decay Rate on Jet-Induced Pressures on a Flat Plate, NASA CR-2979, Apr. 1978.

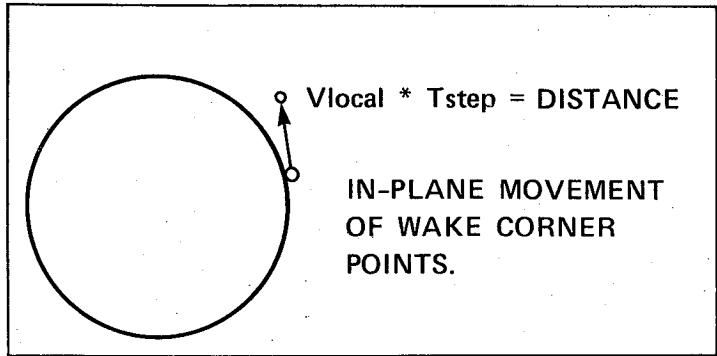
APPENDIX A. The following is a listing of the parameter definition file and the maximum limits definition data file for PMARC.

```
C
C ***** PARAMETER DEFINITIONS *****
C
C     enter: 1 for 1000 panels
C           4 for 4000 panels
C     PARAMETER (NDIM = 4)
C
C     enter: 1   for 1000 wake panels
C           4   for 4000 wake panels
C     PARAMETER (NRPDIM = 4)
C
C     enter: 1 for 50 wake columns
C           4 for 200 wake columns
C     PARAMETER (NRCDIM = 4)
C
C     enter: 1 for 10 wakes
C           5 for 50 wakes
C     PARAMETER (NRDIM = 5)
C
C     enter: 1 for 500 panels/patch
C           2 for 1000 panels/patch
C     PARAMETER (NPPDIM = 2)
C
C     enter: 1 for 100 patches
C           2 for 200 patches
C     PARAMETER (NPDIM=1)
```

```

C
C ***** MAX DATA INPUT *****
C
C current limit on number of wake lines           51/201
  DATA NWLMX / 201 /
C current limit on number of wake-grid-planes     31
  DATA NWGPMX / 31 /
C current limit on number of regions              20
  DATA NREGMX / 20 /
C current limit on number of wake columns         50/200
  DATA NWCMMX / 200 /
C current limit on number of wake points in a set 500/1000
  DATA NSWPMX / 1000 /
C current limit on number of wake panels         1000/4000
  DATA NWPMMX / 4000 /
C
C max variables from GEOMIN
C
C current limit on number of defined sections     500/1000
  DATA NDSMMX / 1000 /
C current limit on number of chordwise regions   1000/3000
  DATA NRCMMX / 3000 /
C current limit on number of base points         500/1000
  DATA NBPMMX / 1000 /
C current limit on number of panels              1000/4000
  DATA NPNLIM / 4000 /
C current limit on number of panels per patch     500/1000
  DATA NPPMMX / 1000 /
C current limit on number of components          10
  DATA NCTMMX / 10 /
C current limit on number of patches              100/200
  DATA NPHMMX / 100 /
C current limit on number of spanwise region     100
  DATA NRSMMX / 100 /
C current limit on number of regions on a section 20
  DATA NRGMMX / 20 /

```



$V = v3 \quad T = t3$

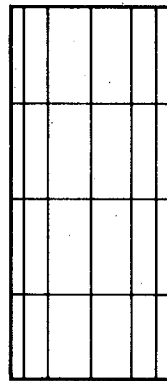
$V = v2 \quad T = t2$

$V = v1 \quad T = t1$

$V = V_j \quad T = 0$



JET WAKE GRID PLANES



SOLID CORE STUB MODEL

Figure 1.- Details of jet relaxation scheme.

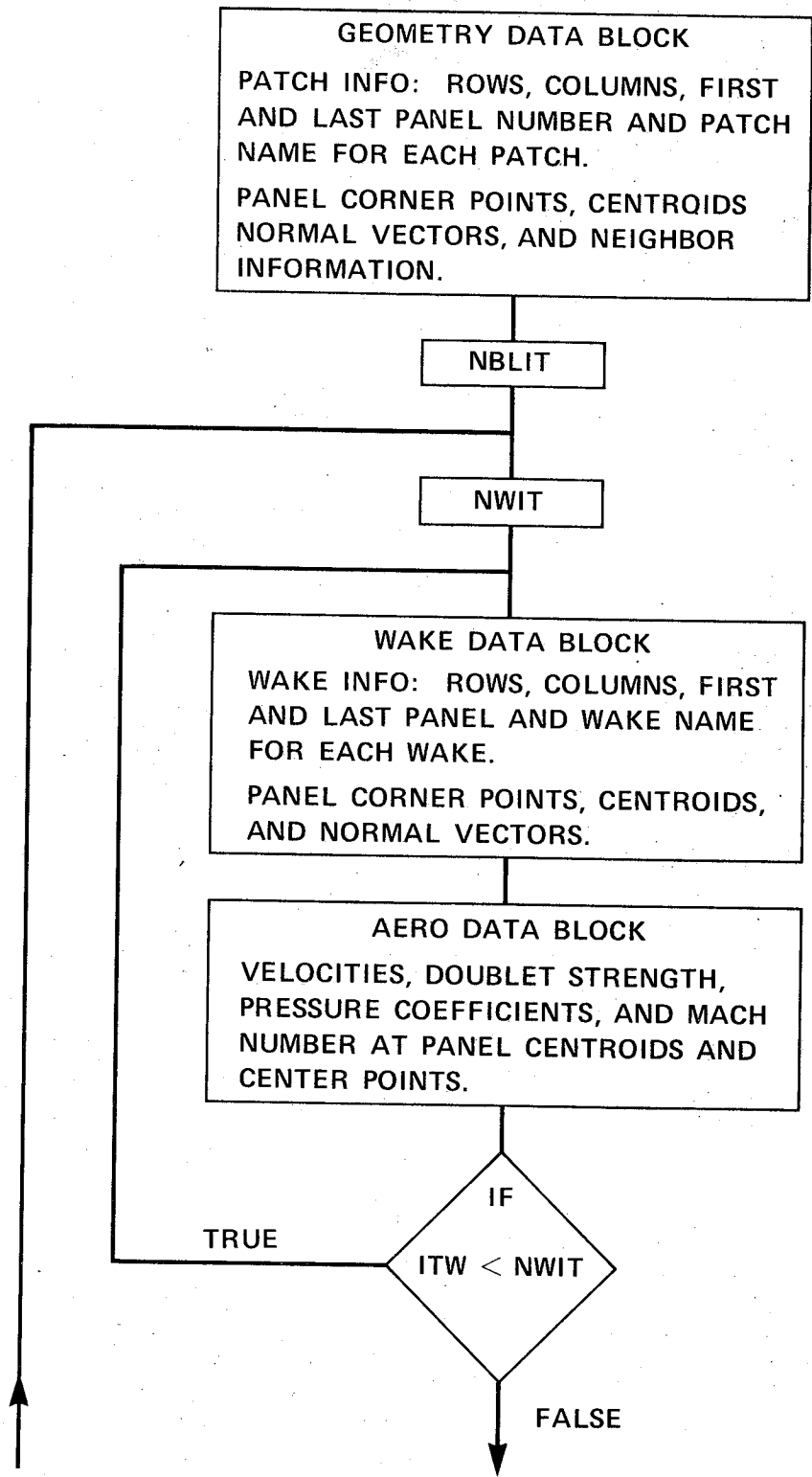


Figure 2.- Data arrangement within PMARC plot file.



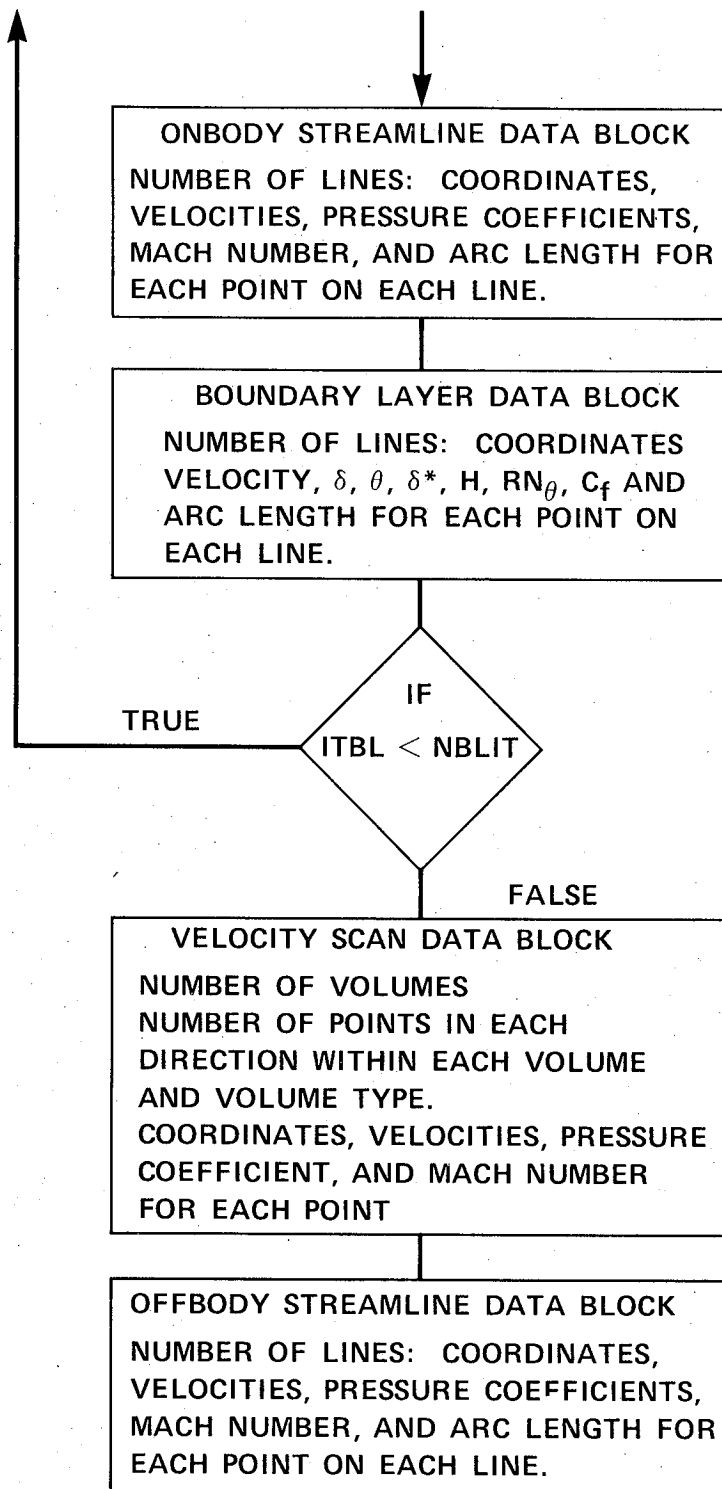


Figure 2.- Concluded.

		COLUMNS				
		1	2	3	4	5
ROWS	1	1            4 (1)	1            4 (6)	1            4 (11)	1            4 (16)	1            4 (21)
	2	1            4 (2)	1            4 (7)	1            4 (12)	1            4 (17)	1            4 (22)
	3	1            4 (3)	1            4 (8)	1            4 (13)	1            4 (18)	1            4 (23)
	4	1            4 (4)	1            4 (9)	1            4 (14)	1            4 (19)	1            4 (24)
	5	1            4 (5)	1            4 (10)	1            4 (15)	1            4 (20)	1            4 (25)

Figure 3.— Panel and corner point numbering sequence within patch.

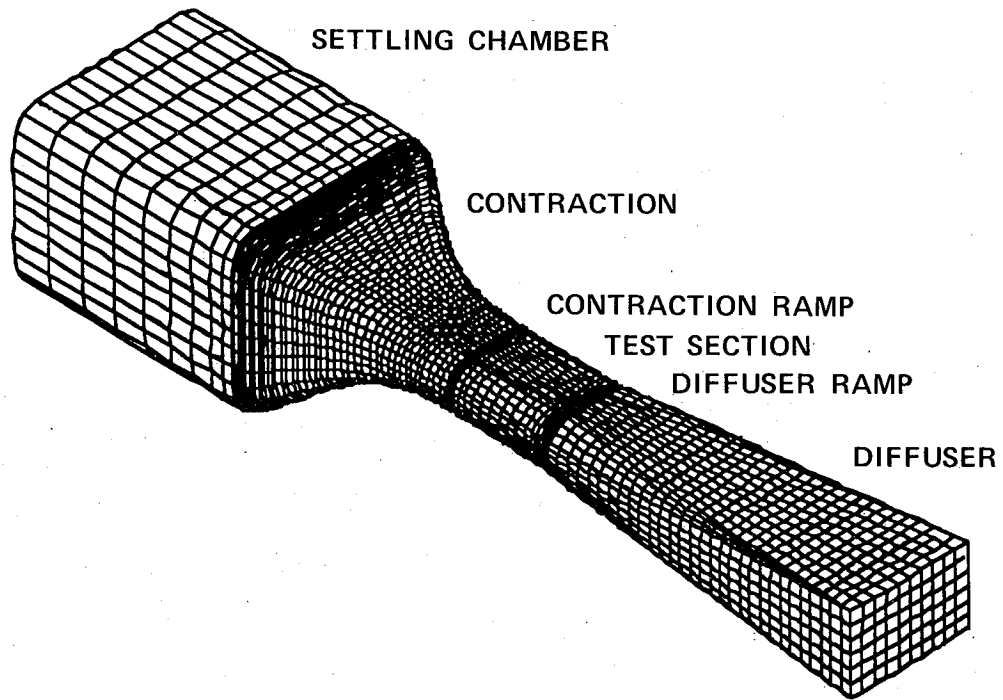


Figure 4.— PMARC paneling of the contraction, test section (including acoustic liner), and diffuser of the 40 x 80 circuit of the NFAC.

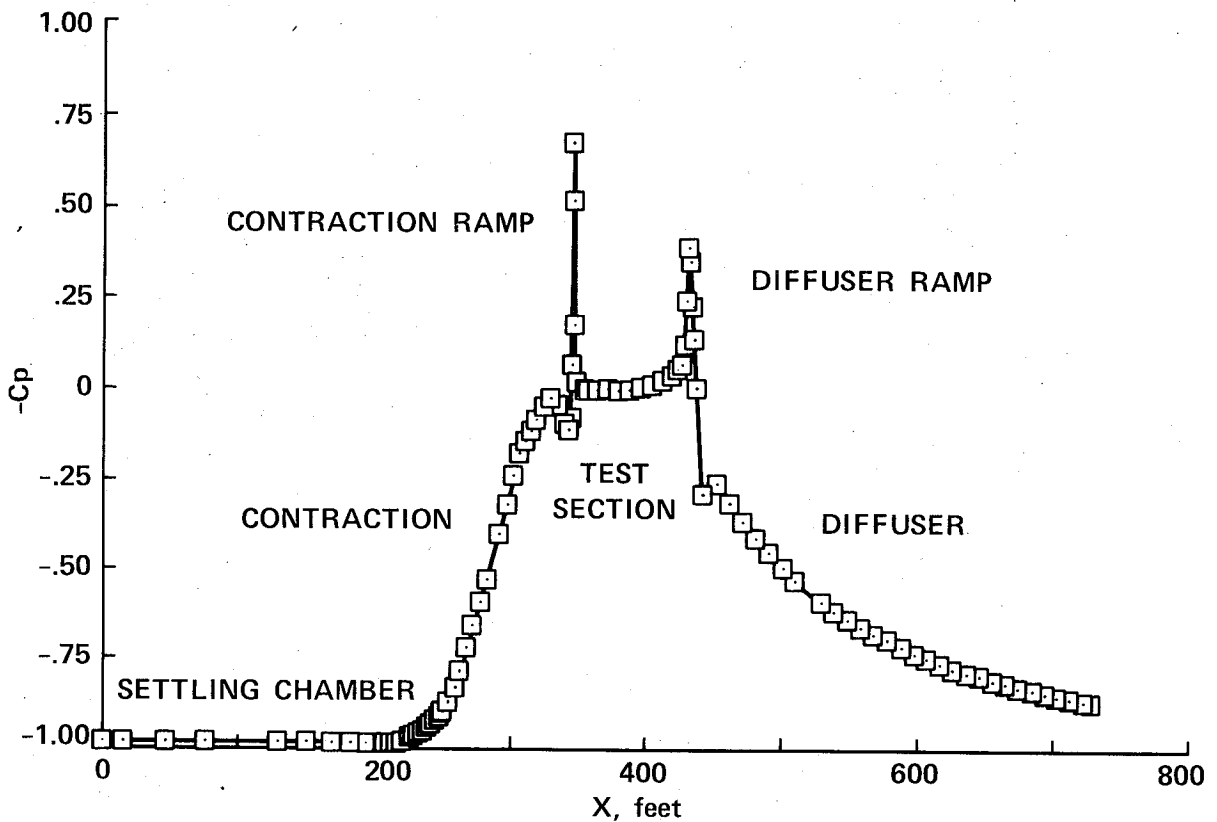


Figure 5.— Wall pressure distribution in 40- by 80-Foot Wind Tunnel as computed by PMARC.

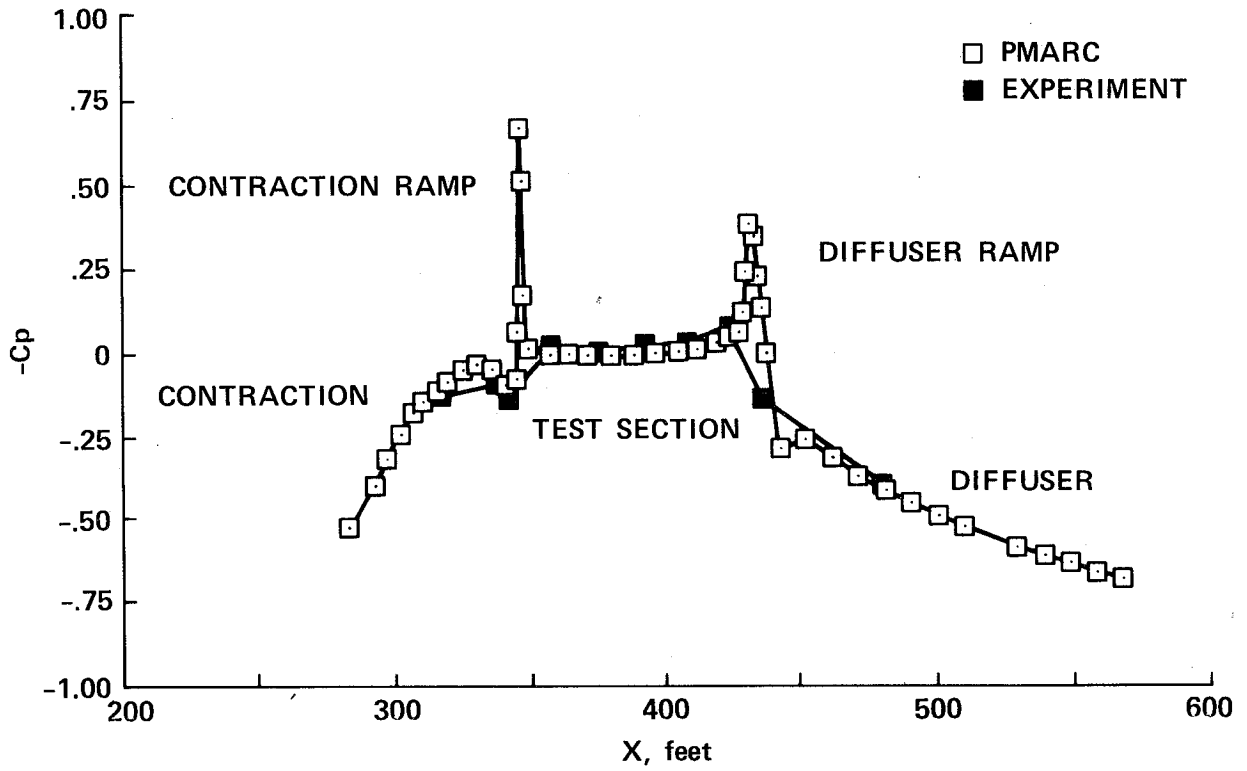


Figure 6.— Comparison of PMARC and experimental wall pressure distributions (full scale) 40- by 80-Foot Wind Tunnel.

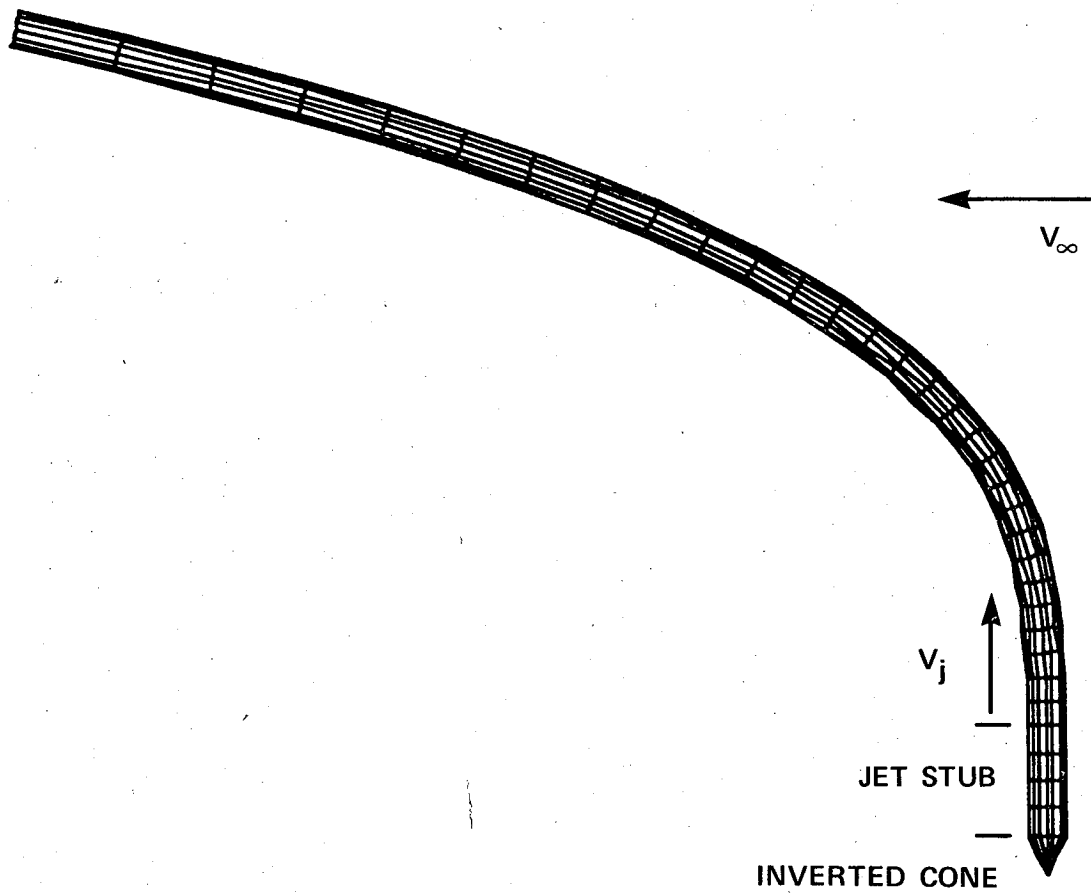


Figure 7.— Jet inclined  $90^\circ$  to the free stream, no wake relaxations, no expansion,  $V_j/V_\infty = 8.0$ .

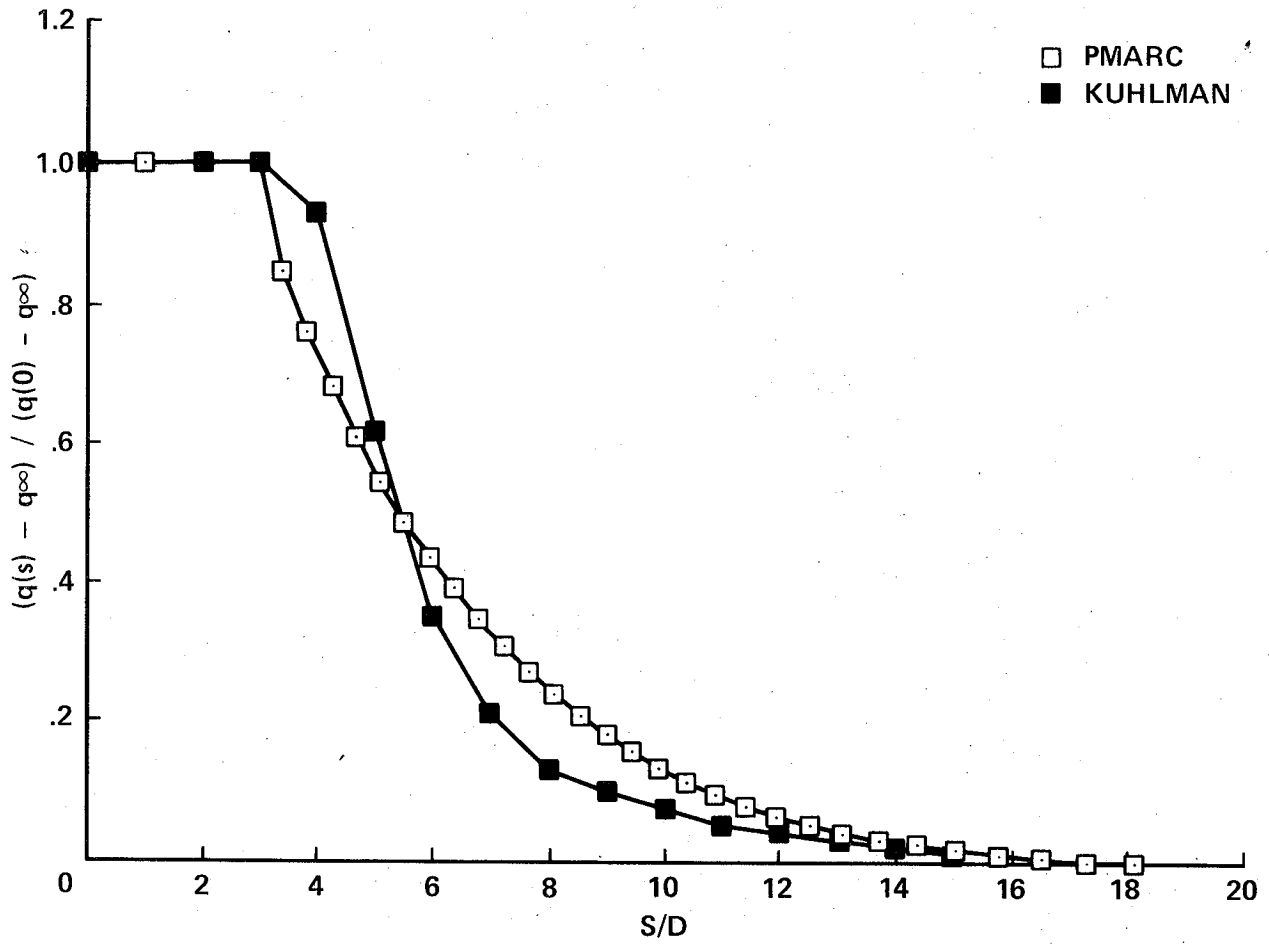


Figure 8.— Dynamic pressure decay along jet trajectory.

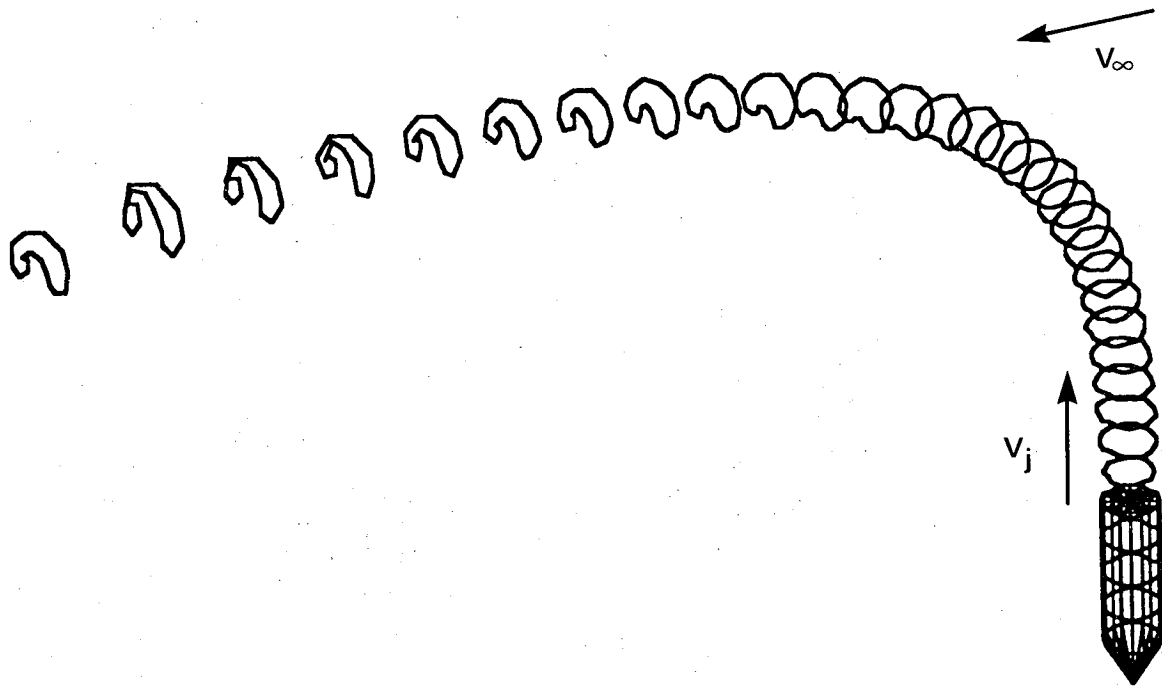


Figure 9.— Jet inclined  $90^\circ$  to the free stream, four wake relaxations, no expansion,  $V_j/V_\infty = 8.0$ .

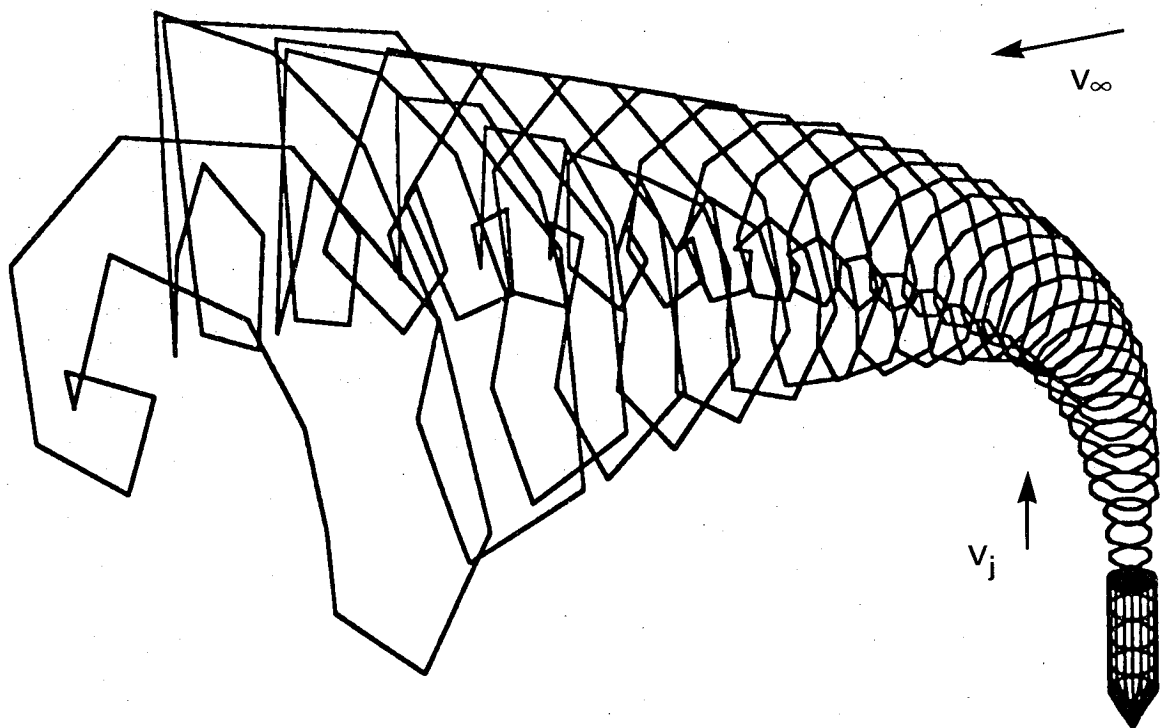


Figure 10.— Jet inclined  $90^\circ$  to the free stream, four wake relaxations, user-defined expansion,  $V_j/V_\infty = 8.0$ .

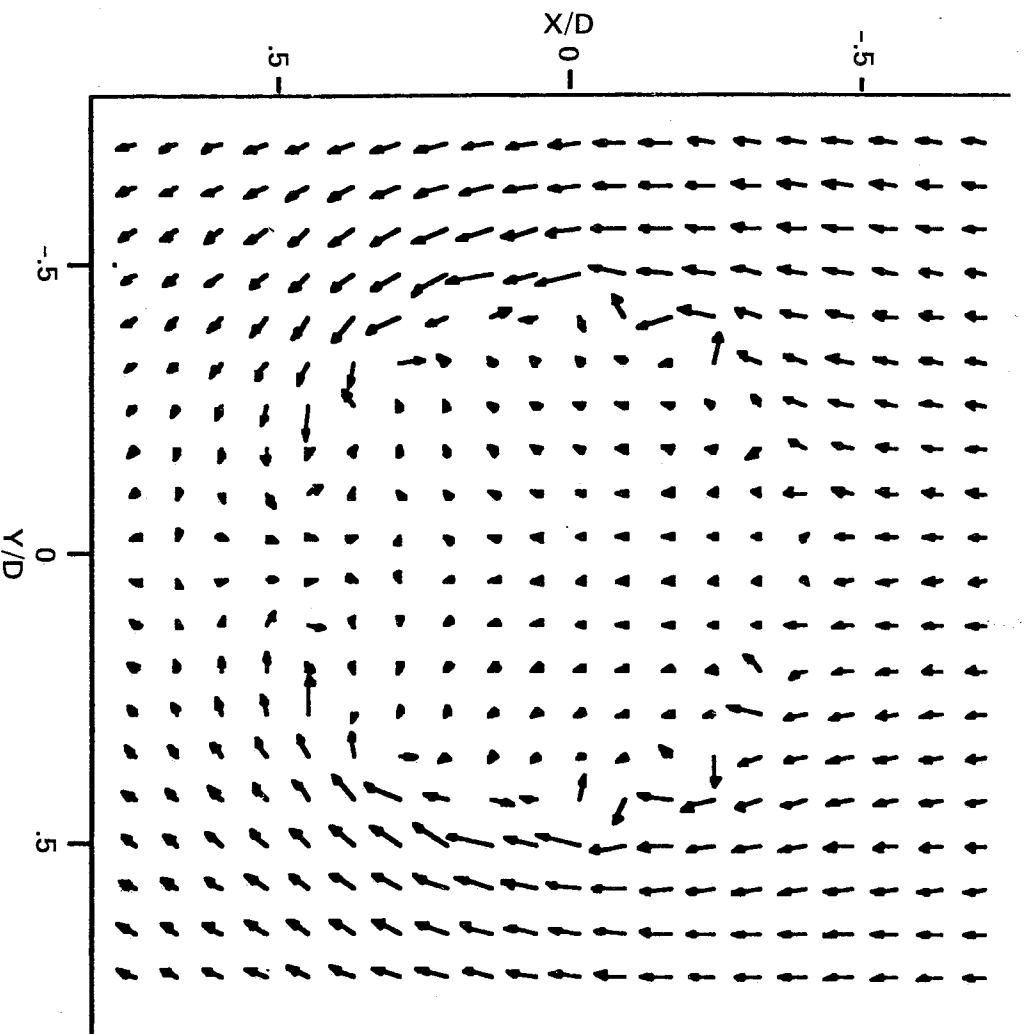


Figure 11.— Velocity scan through jet at  $S/D = 1.15$ ,  $V_j/V_\infty = 8.0$ .



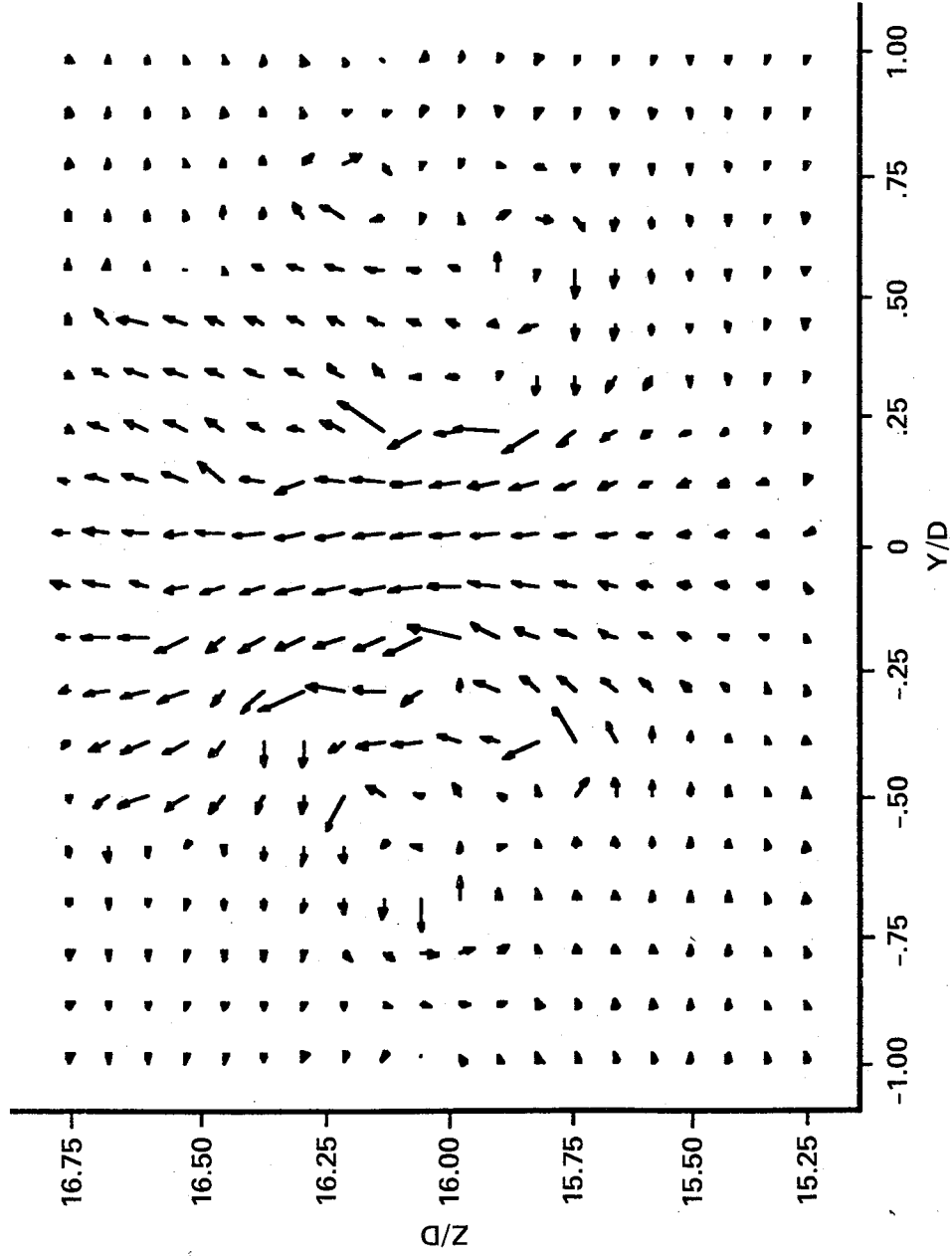


Figure 12.— Velocity scan through jet at  $S/D = 25.0$ ,  $V_j/V_\infty = 8.0$ .

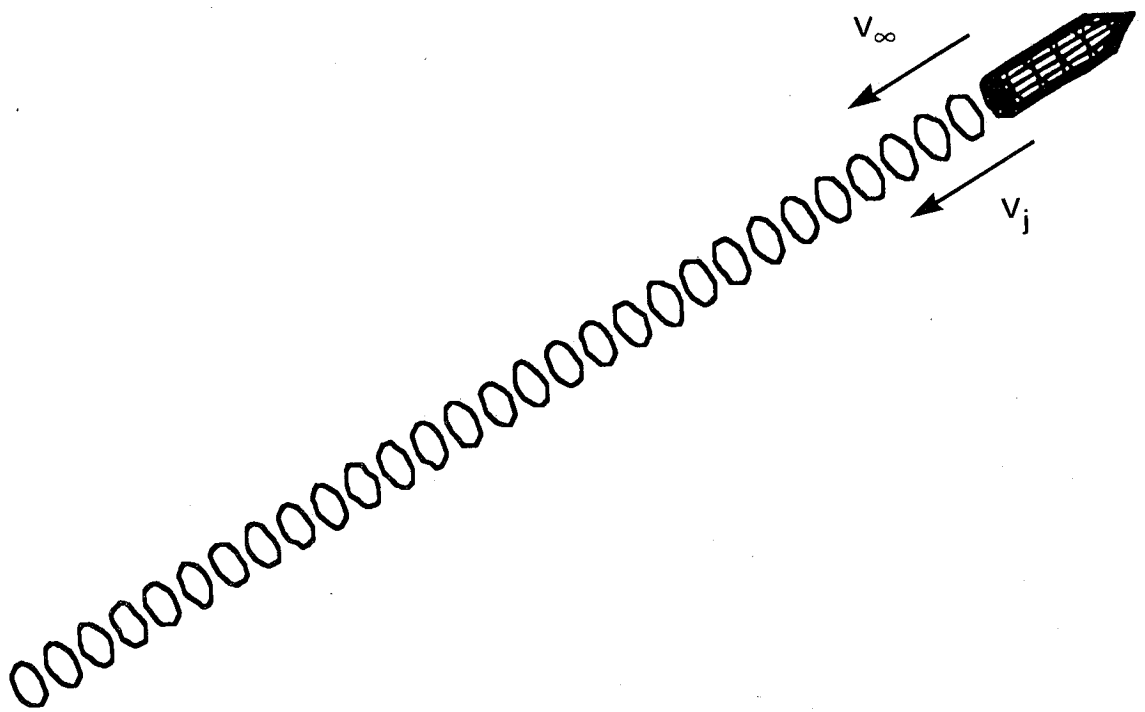


Figure 13.— Jet parallel to the free stream, no wake relaxations, no expansion,  
 $V_j/V_\infty = 8.0$ .

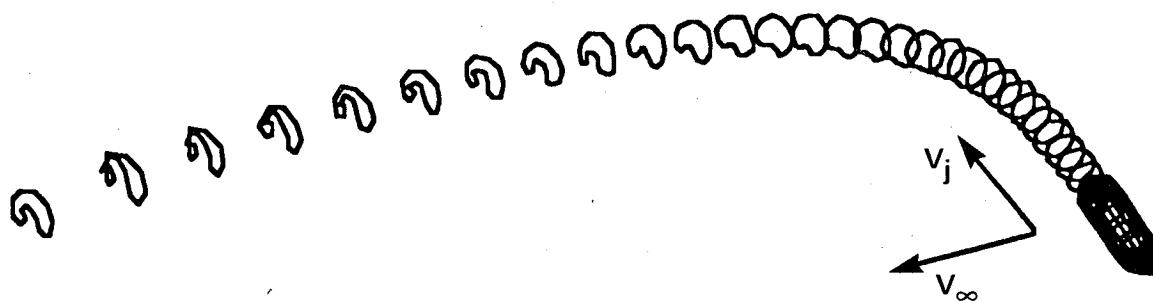


Figure 14.— Jet inclined  $60^\circ$  to the free stream, four wake relaxations, no expansion,  $V_j/V_\infty = 8.0$ .

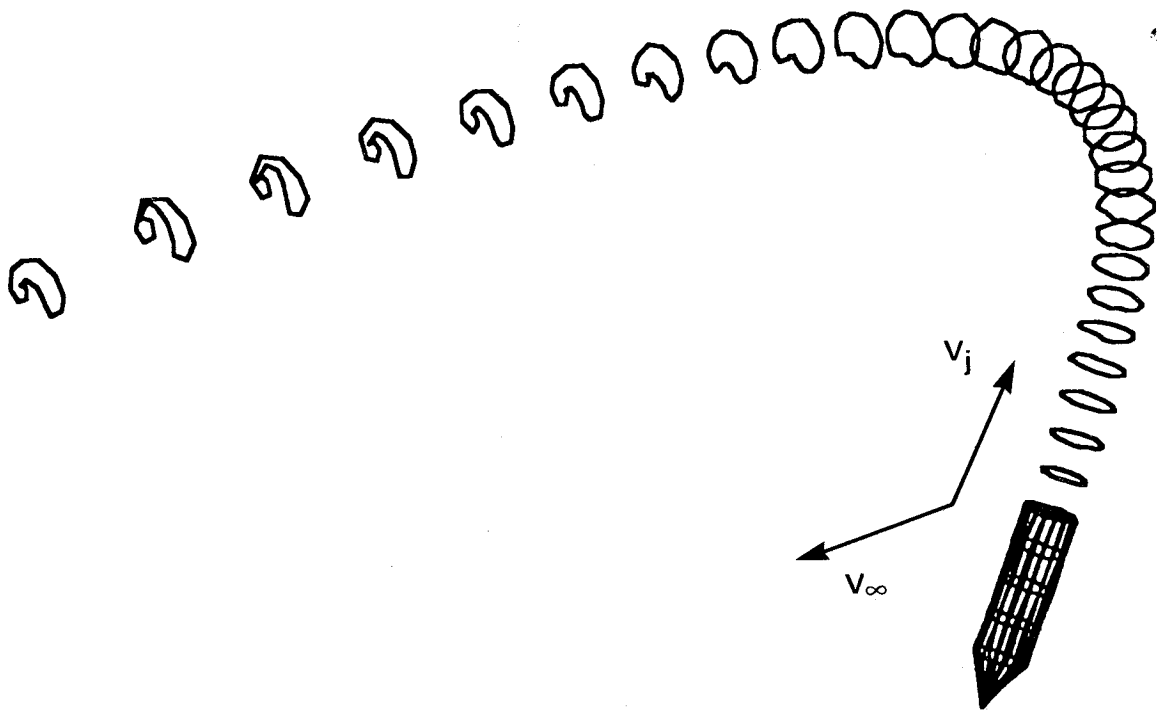


Figure 15.— Jet inclined  $120^\circ$  to the free stream, four wake relaxations, no expansion,  $V_j/V_\infty = 8.0$ .

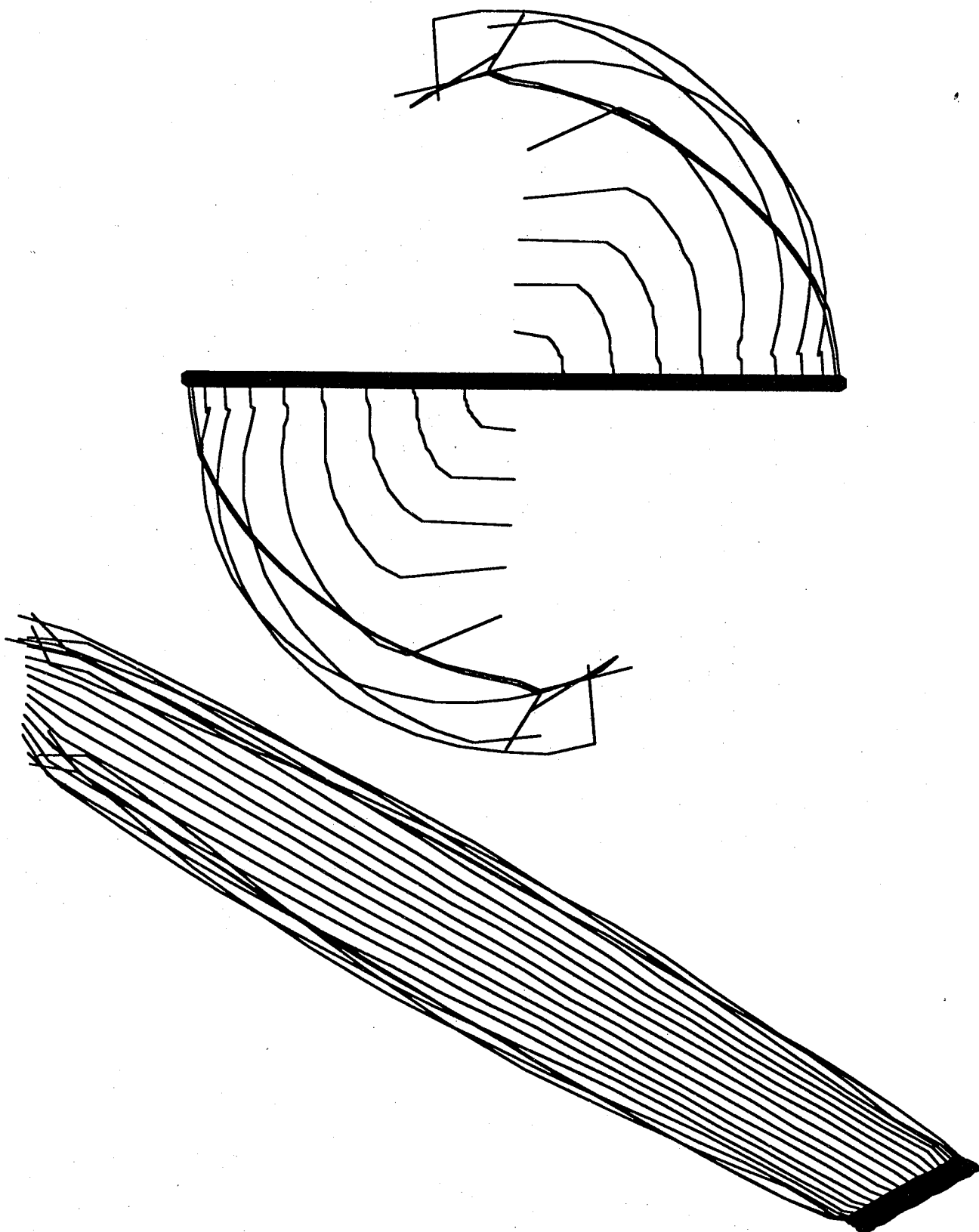


Figure 16.— NACA 0012 wing, AR = 5.0, performing a rolling maneuver  
(front view and three-quarter front view).

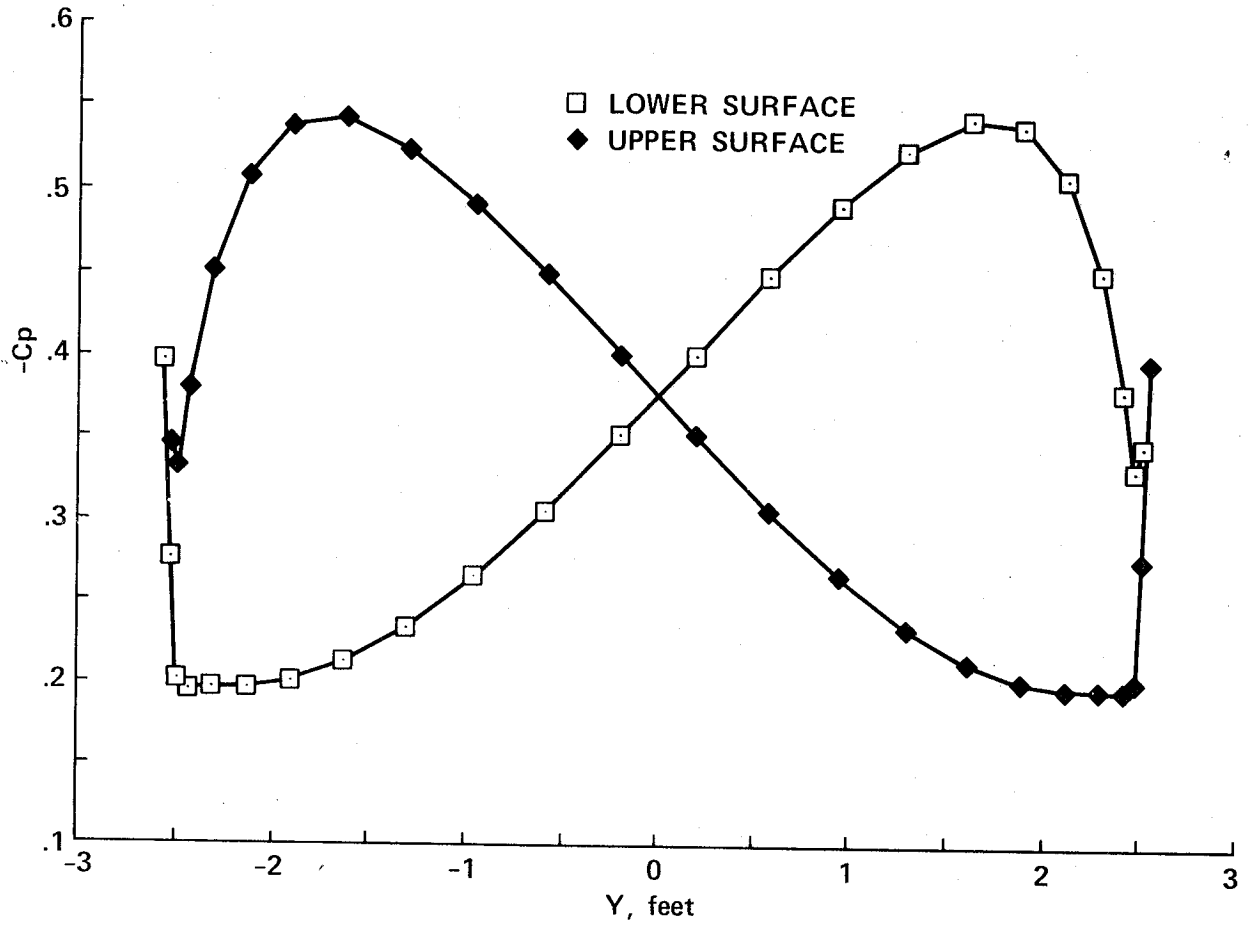


Figure 17.— Spanwise pressure distribution at  $x/c = 0.25$  on a NACA 0012 wing,  $AR = 5.0$ , roll rate =  $3.0^\circ/\text{sec}$ ,  $v_\infty = 1.0 \text{ ft/sec}$ .



# Report Documentation Page

1. Report No. NASA TM-101024		2. Government Accession No.		3. Recipient's Catalog No.	
4. Title and Subtitle  Development and Validation of an Advanced Low Order Panel Method				5. Report Date October 1988	
				6. Performing Organization Code	
7. Author(s)  Dale L. Ashby, Michael R. Dudley, and Steven K. Iguchi (Sterling Federal Systems, Inc., Palo Alto, California)				8. Performing Organization Report No. A-88275	
				10. Work Unit No. 505-61-71	
9. Performing Organization Name and Address Ames Research Center Moffett Field, CA 94035				11. Contract or Grant No.	
				13. Type of Report and Period Covered Technical Memorandum	
12. Sponsoring Agency Name and Address National Aeronautics and Space Administration Washington, DC 20546-0001				14. Sponsoring Agency Code	
15. Supplementary Notes  Point of Contact: Dale Ashby, Ames Research Center, MS 247-2 Moffett Field, CA 94035 (415) 694-5047 or FTS 464-5047					
16. Abstract  A low-order potential-flow panel code, PMARC, for modeling complex three-dimensional geometries, is currently being developed at NASA Ames Research Center. PMARC was derived from a code named VSAERO that was developed for Ames Research Center by Analytical Methods, Inc. In addition to modeling potential flow over three-dimensional geometries, the present version of PMARC includes several advanced features such as an internal flow model, a simple jet wake model, and a time-stepping wake model. Data management within the code has been optimized by the use of adjustable size arrays for rapidly changing the size capability of the code, reorganization of the output file and adopting a new plot file format. Preliminary versions of a geometry preprocessor and a geometry/aerodynamic data postprocessor are also available for use with PMARC. Several test cases are discussed to highlight the capabilities of the internal flow model, the jet wake model, and the time-stepping wake model.					
17. Key Words (Suggested by Author(s)) Panel methods Internal flow Potential flow Powered-lift aerodynamics			18. Distribution Statement  Unclassified-Unlimited  Subject Category - 02		
19. Security Classif. (of this report) Unclassified		20. Security Classif. (of this page) Unclassified		21. No. of pages 46	22. Price A03

